

Elevated Temperature Operation of 4H-SiC Nanoribbon Field Effect Transistors

Min-Seok Kang^a, Jung-Joon Ahn^{a,b}, Anders Hallén^c, Carl-Mikael Zetterling^c, Joseph Kopanski^b and Sang-Mo Koo^a

^a Department of Electronic Materials Engineering, Kwangwoon University, Seoul, Korea, hyde0220@gmail.com

^b Semiconductor and Dimensional Metrology Division, National Institute of Standards and Technology, Gaithersburg, MD, USA

^c KTH Royal Institute of Technology, P.O Box Electrum 229, SE 164 40 Kista, Sweden

Nanoribbon structures have shown considerable potential for low leakage, and a high on/off current ratio with the low power consumption, due to its high surface-to-volume ratio, and small size [1]. Also, Nano-ribbon structures have recently shown promise to enable high-density electronics as well as in high-performance sensors [2]. SiC material has been proposed to replace conventional silicon devices which already are approaching the material limit in power electronics. SiC-based devices exhibit a high-temperature and high-power capabilities [3-4]. The combination of the structural advantages of nanoribbon-based devices and the materials properties of SiC may result in devices with improved performance.

In this work, 4H-SiC nanoribbon FETs have been fabricated by “top-down” approach and the characteristics of the fabricated devices have been studied at the elevated temperature.

We fabricated 4H-SiC nanoribbon FETs with various channel thickness (t_{CH}) of 100 and 200 nm, respectively. The reference samples were also prepared: a T_{CH} of $\sim 0.5 \mu\text{m}$. Fig. 1 shows the schematic view of the 4H-SiC nanoribbon FETs. The starting materials are p-type 4H-SiC wafers ($N_A=1\times 10^{18} \text{cm}^{-3}$) with a n-type epilayer ($N_D=1\times 10^{18} \text{cm}^{-3}$). The channels were defined further by a photolithography and etch process. A ~ 50 nm-thick Ni layer has been patterned with a lift-off process. After that, inductively coupled plasma (ICP) etch process employing the Ni metallization as an etch mask to form the SiC channel and the wide Source/Drain (S/D) regions simultaneously. The length L_{CH} and width W_{CH} of the channels were $10 \mu\text{m}$ and $3 \mu\text{m}$, respectively. The S/D contacts of Ni/Al with the thickness ratio of 0.2/0.8 were deposited. Ni has been used as metal electrode for the backside gate contact. The samples were annealed at $900 \text{ }^\circ\text{C}$ in N_2 for 90s for Ohmic contact. Finally, the top Au gate was defined by a photolithography and lift-off process.

The fabricated devices were examined by using field emission scanning electron microscopy (FE-SEM) and atomic force microscopy (AFM), respectively. Current-voltage I - V characteristics of the device were measured by using a Keithley 4200 semiconductor parameter analyzer for comparison at different temperature ranges. The experimental results have also been compared with numerical simulation results obtained from structures identical to those of the fabricated devices. In order to evaluate the back gate and top gate bias-dependent channel carrier modulation as a function of temperature, we extracted the channel cross-section profiles containing the on- and off-current density distribution.

The 4H-SiC nanoribbon FETs show normally-on characteristics, as shown in Fig. 2. The channel can be depleted and turned-off by applying negative bias on the Schottky gate of the FETs. On the other hand, a positive gate bias increases the channel current by decreasing the depletion region. The threshold voltage V_{th} of the nanoribbon FET ($t_{CH} = 100 \text{ nm}$) observed a positive shift compared to that of the reference ($\Delta V_{th} = 12.5 \text{ V}$). The fabricated nanoribbon FET shows the improved gate control.

The measured I_D - V_G characteristics at various measurement temperatures from 300K to 500K are shown in Fig. 3. It is observed that the V_{th} of the fabricated FETs show a negative shift with the measurement temperature increases. The threshold voltage variation of the SiC nanoribbon FET is lower than that of the reference FET, which means the nanoribbon FETs are more stable at high temperature, as shown in Fig. 4.

These results suggest that the proposed SiC nanoribbon structures significantly improve the gate control at high temperatures and thereby making them promising for high-temperature sensing testbeds.

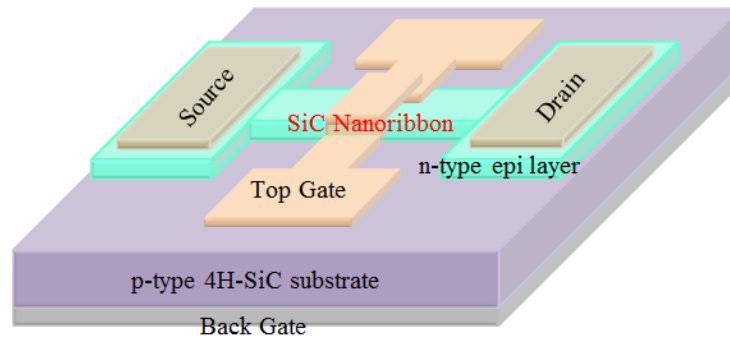


Fig.1 Schematic view of the 4H-SiC nanoribbon FET.

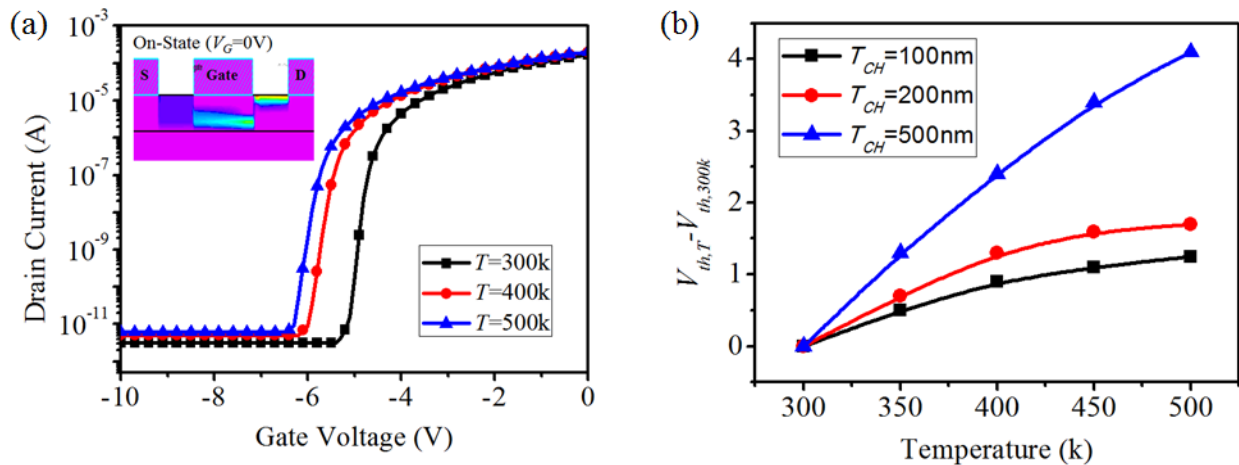


Fig.2 (a) I_D - V_G characteristics and current density distribution of a 4H-SiC nanoribbon FET ($t_{CH} = 100$ nm) at different temperatures and (b) Threshold voltage variation of the 4H-SiC nanoribbon FETs and a reference FET at different temperatures.

References

- [1] J. Y. Mori and H. Kohno, Nanotechnology 20 (2009) 285705-285708.
- [2] J.-H. Choi, L. Latu-Romain, T. Chevolleau, T. Baron, and E. Bano, Materials Science Forum 893 (2012) 717-720.
- [3] J. Zhuge, Y. Tian, R. Wang, R. Huang, Y. Wang, B. Chen, J. Liu, X. Zhang, and Y. Wang, IEEE Transactions on Nanotechnology, 9 (2010) 114-122.
- [4] A. Saha, and James A. Cooper, IEEE Trans. Electron Devices 54, p.2786 (2007)